Statistik turbulenter Rohrströmungen über einen Reynoldszahl-Bereich von $5 \cdot 10^4$ bis $2 \cdot 10^5$

Turbulent Pipe Flow Statistics over Reynolds Number Range of $5 \cdot 10^4$ – $2 \cdot 10^5$

S. Richter[1], E.-S. Zanoun[1], J. Peixinho[2], C. Egbers[1]
[1] Department of Aerodynamics and Fluid Mechanics, BTU Cottbus-Senftenberg, Cottbus, Germany
[2] Laboratoire PIMM, CNRS, Arts et Metiers Institute of Technologie, Paris

Schlagworte bitte hier in Deutsch Rohrströmung, Turbulenz, Statistik turbulenter Strömung
Key words in English here Pipe flow, turbulence, statistics of turbulent flow

Abstract

To explore pipe flow structures in fully developed turbulent flow regime, the present study characterises velocity statistics over a relatively wide range of Reynolds numbers $5 \cdot 10^4 \leq Re \leq 2 \cdot 10^5$. New sets of experiments were performed in the CoSma-Pipe facility available at the Department of Aerodynamics and Fluid Mechanics, BTU C-S, utilizing hot-wire anemometry. The turbulence statistics were investigated from the pipe near-wall to the pipe centreline. Recent direct numerical simulations have been used for direct comparison of the detailed experimental results such as the mean velocity profile, variance, skewness and flatness factors, as well as peak value and location of the streamwise normal Reynolds stress component.

Introduction

Wall-bounded shear flows are characterized by a wide range of turbulence interacting length scales. Small-scale structures, for instance, control the overall behavior of such turbulent shear flows. Small scales of turbulent flows dissipate the turbulent kinetic energy into heat in large parts of the flow. On the other hand, the inner peak of the large scale, i.e., energy-containing, structures are formed due to the dynamics of turbulent fluctuations within the viscous sublayer. Thus, intensive research work has been devoted towards turbulent flow structures within the wall layer over decades in ducted, i.e. pipe and channel, as well as flat plate boundary layer flows, see e.g. Cantwell 1983. It is, however, of crucial importance in such wall-bounded shear flows studies to consider the spatial resolution of the velocity measuring probe size to investigate turbulent flow statistics. It is also common to express its influence on measured velocity data in wall units, i.e. in terms of ℓ^+ where $\ell^+ = \ell u_\tau / \nu$, ℓ is the length of the measuring probe, u_τ is the wall friction velocity, and ν is the kinematic viscosity, see Tab. 1. When it is not into account it results in measurements inaccuracies, in particular, at high Reynolds numbers in the wall vicinity, see e.g. Ligrani and Bradshaw 1987, Wei and Willmarth 1989, Gad-el-Hak and Bandyopadahyay 1993. Thus, we intend in this short piece of work to highlight turbulent pipe flow statistics over a Reynolds Number range of $5 \cdot 10^4$ to $2 \cdot 10^5$ using commercial thermal probes, however, we are indeed still progressing aiming at NSTAB probes to better resolve the inner as well as the outer peaks of the pipe large-scale structures at LAS, BTU C-S.

GALA e.V., Karlsruhe, Germany, ISBN 978-3-9816764-7-1

Experimental Setup

The measurements presented were conducted at the chair of Aerodynamics & Fluid Mechanics at BTU Cottbus-Senftenberg using the so-called Cottbuser Small Pipe (CoSma Pipe) depicted in Fig. 1. The CoSma Pipe is an open-loop, subsonic pipe test facility covering a Reynolds Number Range of $10^4 \leq Re_b \leq 2x10^5$ which has been built to provide experimental data, complementing the on-going investigations of the Cottbuser Large Pipe (CoLa Pipe) turbulence characteristics at high Reynolds numbers. The facility consists of a 1.2 m long settling chamber with a contraction ratio of 12.25, a 9.5 m long pipe section made of acrylic and borosilicate glass respectively depending on the type of experiments conducted inside the facility.

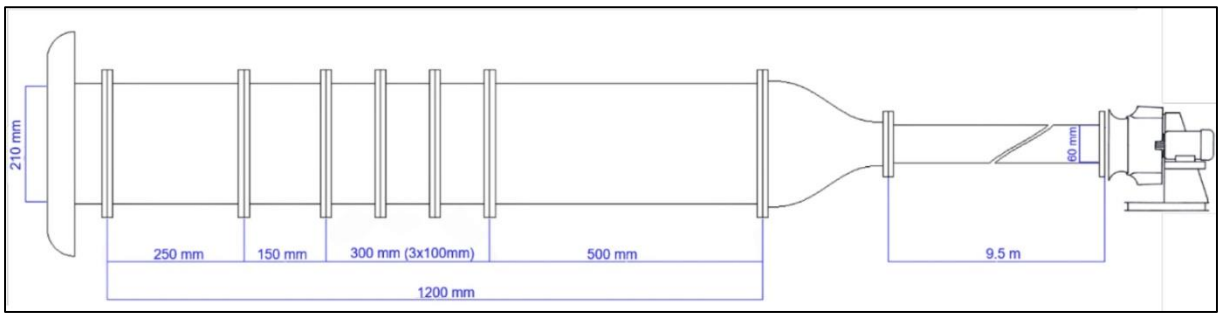

Figure 1: Schematic of the open-loop test facility CoSma-Pipe

The flow properties of five Reynolds number cases examined are shown in Tab. 1. The measurements were conducted in a reasonable distance from the settling chamber with a length-to-diameter ratio (L/D) of 130 to ensure a fully developed turbulent flow. The experimental data sets were obtained by the use of a Dantec 55P15 1D boundary layer hot-wire probe connected to a constant temperature anemometer (CTA) Dantec Stream-Line system. Due to the pipe's small diameter of 6 cm and its corresponding curvature compared to the relatively long length of the used hot wire, for most measurements it was not possible to resolve the viscous sub layer, parts of the buffer layer and its corresponding inner peak. Tab. 1 addresses the minimum distance to the wall (y^+_{min}) that could be resolved. As an exception serves the case of $\mathrm{Re}_\tau = 2{,}316$ which was done in the beginning of this campaign which gave the impression that also the subsequent experiments could be resolved in the same manner. Afterwards, it turned out that this hot wire possessed slightly tilted prongs but, unfortunately, was destroyed in the process of another measurement campaign and could not be repaired to the same ability. This problem will be solved by the use of a miniaturized hot wire system which is planned to be purchased soon and, therefore, it is the author's objective to complete the here presented experiments shortly after. Furthermore, the presented measurements are compared to two DNS data sets of Re_τ = 1,500, see Bauer et al. 2017, and Re_τ= 3008, see Ahn et al. 2015.

Table 1: Examined Reynolds numbers and flow properties

No.	U_{bulk} [m/s]	Re_b [-]	u_τ [-]	Re_τ [-]	ℓ_c [µm]	ℓ^+ [-]	y^+_{min} [-]
1	12.5	50,000	0.645	1260	23.87	52.15	35
2	14.8	60,000	0.748	1450	20.68	60.46	47
3	25.66	100,000	1.19	2316	12.95	95.31	6
4	36.9	150,000	1.67	3205	9.36	133.56	32
5	50.21	200,000	2.2	4190	7.23	172.86	46

$\ell_c = \nu/u_\tau$ viscous length scale, and ℓ^+ is the hot-wire length in wall units.

Flow quality

Before the measurement's analysis is addressed, a short overview of the flow quality of the pipe facility shall be given. Fig. 2 and Fig 3. show the characteristics of the pipe's contraction nozzle and its laminarisation capability. In the following the terms contraction exit and pipe inlet can be regarded as a synonym to each other as they represent the same location within the pipe. Fig. 2 shows the turbulence intensity at the contraction exit and pipe inlet respectively. The streamwise turbulence intensity defined as $TI = \frac{\sqrt{u'^2}}{\bar{U}}$, based on the velocity fluctuation u' and the mean velocity $\bar{U}$, was measured by the use of a hot wire anemometry system having the hotwire positioned at the centre of the contraction outlet with increasing velocities ranging from 2.2 m/s up to 22.5 m/s. The result shows a reasonable behaviour keeping the turbulence intensity lower than 1% for a Reynolds number region ranging from 1,500 up to 85,000 with the Reynolds number defined as $Re = \frac{\bar{U} \cdot d}{\upsilon}$, with d as the pipe's diameter and ν as the kinematic viscosity. The deviation of the velocity profile defined as $\frac{U_{local} - \bar{U}}{\bar{U}}$, given in per cent, is presented in Fig. 3 showing a uniform pattern by keeping the deviation from $\bar{U}$ below 1% with *y* representing the wall-normal distance. The underlying data acquisition was conducted by the use of a static Pitot tube that was moved in spatial direction along the whole diameter of the pipe inlet from one wall to the opposite one.

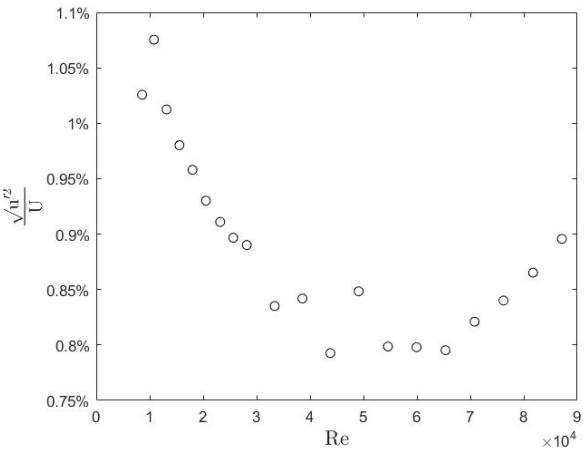

Figure 2: Turbulence intensity at the contraction exit / pipe inlet

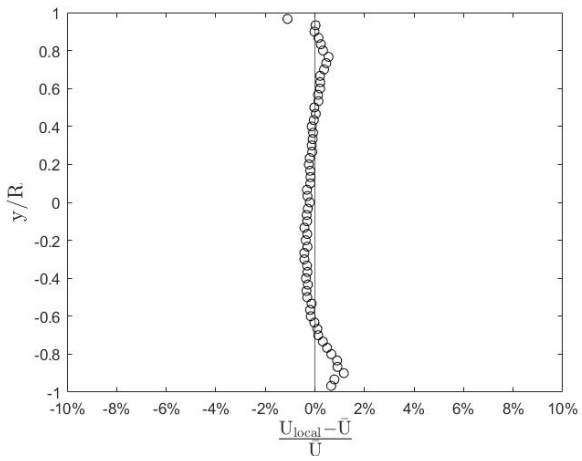

Figure 3: Deviation of the mean velocity profile at contraction exit / pipe inlet

Results and analysis

Streamwise mean velocity profile

In the present study, the streamwise velocity component in pipe flow was measured using hot-wire anemometry with commercial probes from Dantec Dynamics. The streamwise mean velocity profile given in Fig. 4 shows a satisfactory agreement for all five cases presented with the logarithmic law of the wall, $\bar{U}^+ = \frac{1}{\kappa} \ln y^+ + B$, where κ = 0.39 and *B* = 4.42, see Perry et al. 2001, representing the behaviour of the mean velocity profile within the logarithmic region. It presents the normalized local streamwise mean velocity component $\bar{U}^+ = \bar{U}/\mathrm{u}_\tau$ versus the normalized wall-normal distance $y^+ = \mathrm{y}\mathrm{u}_\tau/\nu$, here y is the wall-normal distance, ν the fluid kinematic viscosity and u_τ the wall friction velocity defined as $\mathrm{u}_\tau = \sqrt{\tau_w/\rho}$, with τ_w as the wall shear stress and ρ the fluid density.

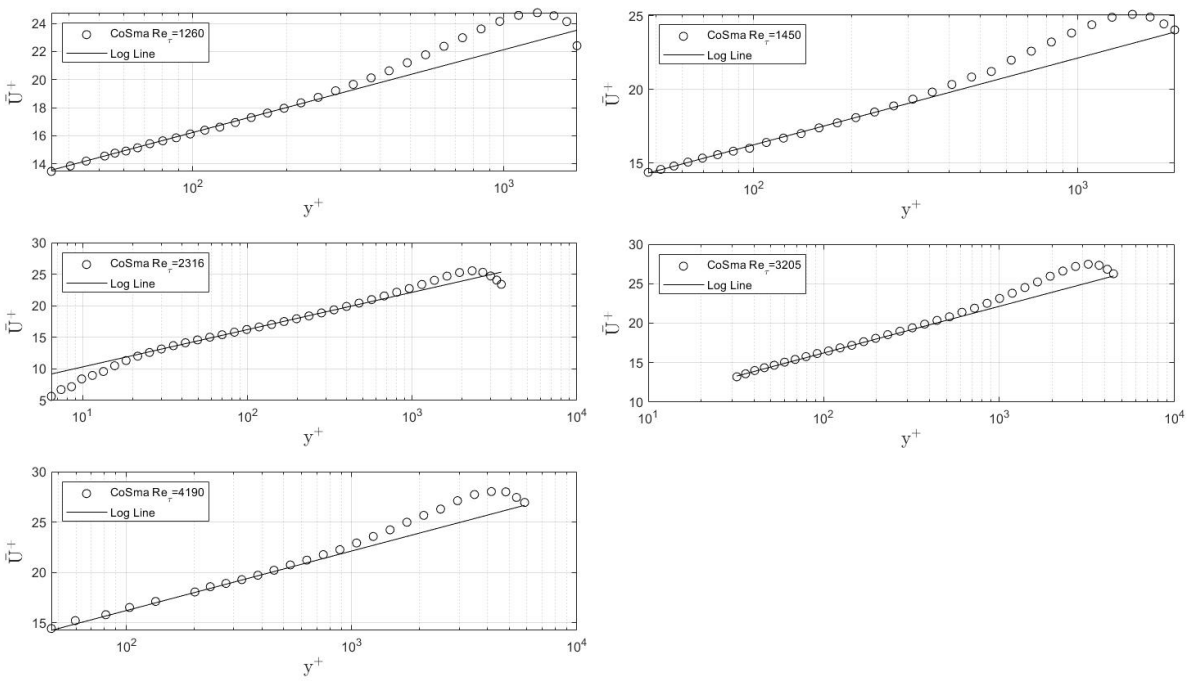

Figure 4: The normalized streamwise mean velocity profile compared to the logarithmic law of the wall $\overline{U}^+ = \frac{1}{\kappa}\ln y^+ + B$, where κ = 0.39 and B = 4.42, see Perry et al. 2001

Streamwise normal stress

The distribution of the streamwise normal Reynolds stress component, u'^2, in pipe flow at different Reynolds numbers is presented in Fig. 5. It is worth noting here that the present results of streamwise velocity fluctuations presented obtained without tripping the flow at the pipe inlet, however, corrected for spatial resolution effect of the wire length, see Smits et al. 2011.

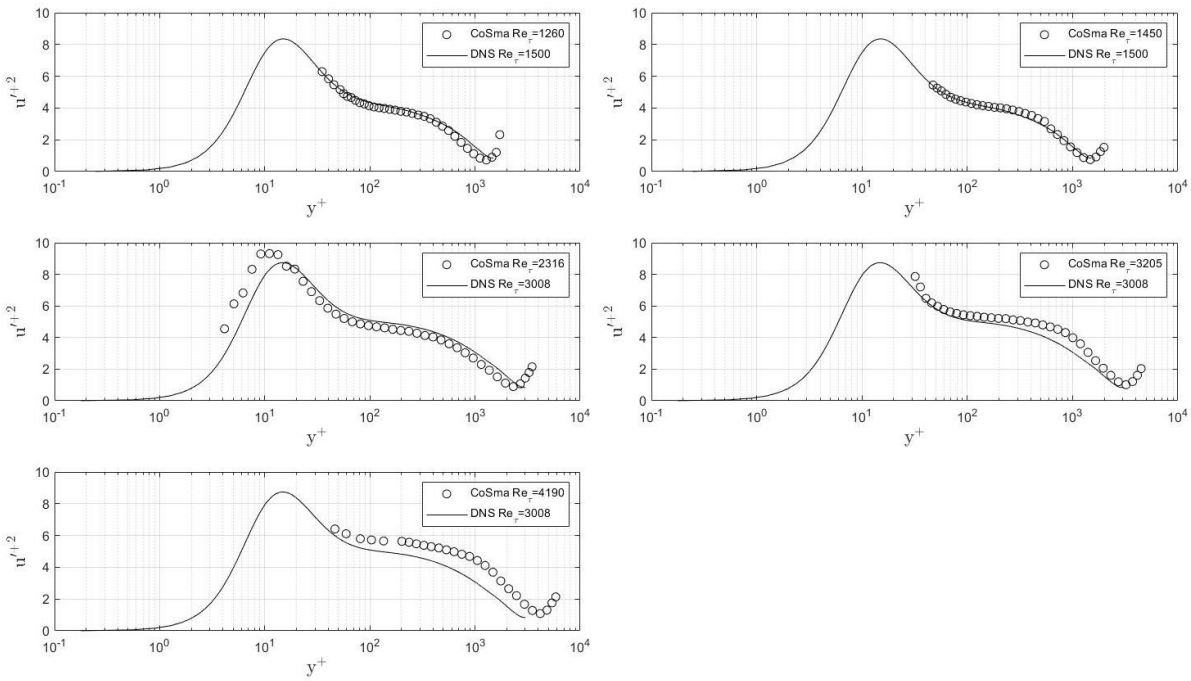

Figure 5: The normalized streamwise normal Reynolds stress component compared with DNS data.

GALA e.V., Karlsruhe, Germany, ISBN 978-3-9816764-7-1

The data in Fig. 5 are normalized with the shear velocity, u_τ, to give $u'^2=(u'/u_\tau)^2$, and the wall distance normalized with the viscous length scale to yield $y^+=y\,u_\tau/\nu$. The normalized data using wall variables indicate that there is a Reynolds number dependence in both the wall layer and also in the core region. Fisher et al. [2001] concluded that a sink term in the dissipation rate equation is responsible for such Reynolds number dependence in the wall region and away from the wall the Reynolds number dependence originates from the streamwise pressure gradient. The figure also clearly indicates the maximum inner peak in the neighbourhood of $y^+=15$ with a maximum value between 8 and 10, depending on the Reynolds number, being in good agreement with Direct Numerical Simulation (DNS) data sets for $Re_\tau = 1{,}500$ and $Re_\tau = 3{,}008$. One might also observe that the velocity fluctuations are decaying as the distance from the wall increases; however, the rate of decaying is decreasing with increasing Reynolds number which might be attributed to intermittency effect which increases with increasing Reynolds number. A lack of data in the viscous region is recognisable and will be addressed in a new measuring campaign using the NSTAB probes. Nonetheless, the agreement between experimental and DNS data is observed.

The centreline velocity fluctuations for fully developed pipe flow regime were measured for different Reynolds numbers showing the CoSma Pipe's experimental data being in good agreement with the compared data presented in Fig. 6. The figure presents the turbulence intensity level at the pipe centreline compared to data extracted from the literature, showing a monotonic decrease as the centreline-based Reynolds number, Re_c, increases. It was documented by Zanoun 2003 that in pipe core region, particularly, at the centreline the streamwise velocity fluctuations are proportional to the wall friction velocity. On the other hand, the wall friction velocity is directly proportional to the square root of the streamwise mean pressure gradient, d*p*/d*x*, and the centreline velocity is directly proportional to the streamwise mean pressure gradient. As a result, with increasing Reynolds number the rate of increase of the centreline mean velocity is greater than the rate of increase in the centreline velocity fluctuations resulting in a decrease in the centreline turbulence intensity level with increasing Reynolds number.

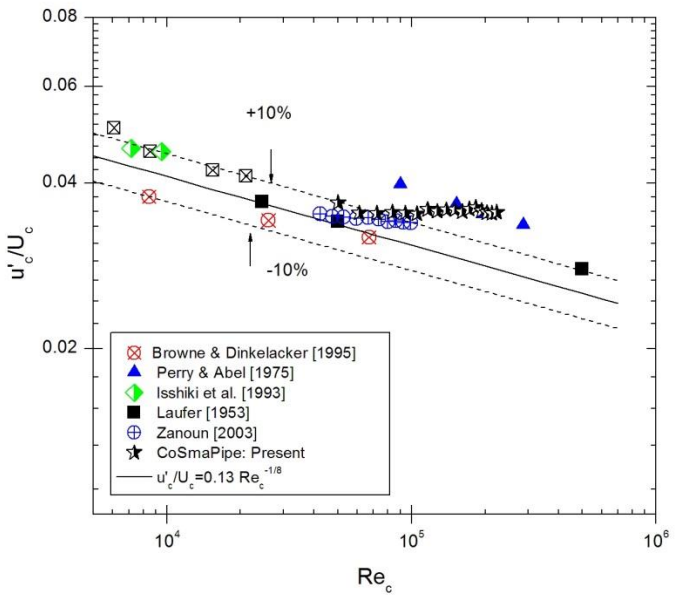

Figure 6: The centerline normalized streamwise turbulence intensity versus centerline-based Reynolds number for fully developed pipe flow regime. Comparison with other authors.

Higher order statistics

In order to meet the requirements of acquiring enough data to obtain reliable skewness and flatness factors, 4x10^6 data samples with a frequency of about 32 kHz have been implemented. The skewness S_u and F_u flatness factors are defined as $S_u(u') = u_c'^3/(u_c'^2)^{3/2}$, and $F_u(u') = u_c'^4/(u_c'^2)^2$ respectively. The comparison between experimental and the DNS data has been made only for $Re_\tau = 3{,}008$.

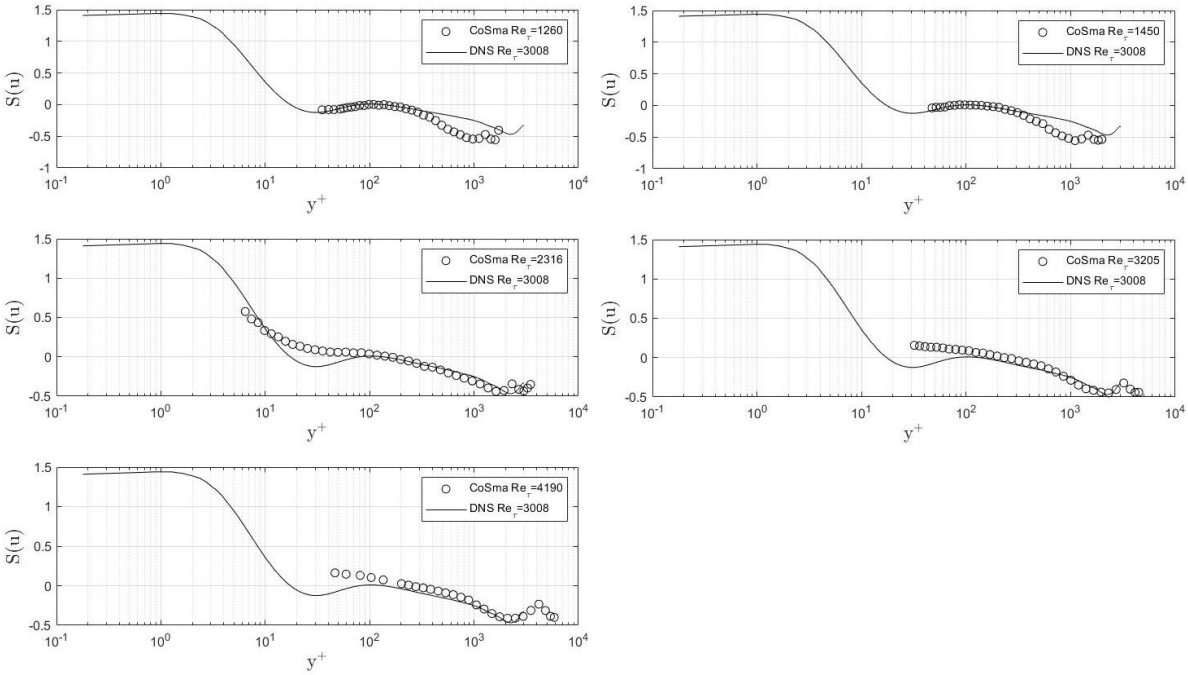

Figure 7: Skewness of experimental and DNS data, see Ahn et al. 2015.

Figure 7 shows a qualitative agreement with DNS data, except in the wall vicinity where the resolution of the hot wire probe was not high enough to resolve the inner layer of present measurements. However, surprisingly, the experimental data for the two lowest cases follow the DNS data illustrated better agreement with regard to the typical decrease of the skewness factor within the region of $\boldsymbol{y}^+ \approx 20$ to ≈ 100 whereas the three higher experimental cases seem not to indicate this behaviour and remain right skewed at $\boldsymbol{y}^+ \approx 100$. Due to the closer proximity of the latter cases to the DNS data, both data sets collapse very well close to the pipe's centreline.

GALA e.V., Karlsruhe, Germany, ISBN 978-3-9816764-7-1

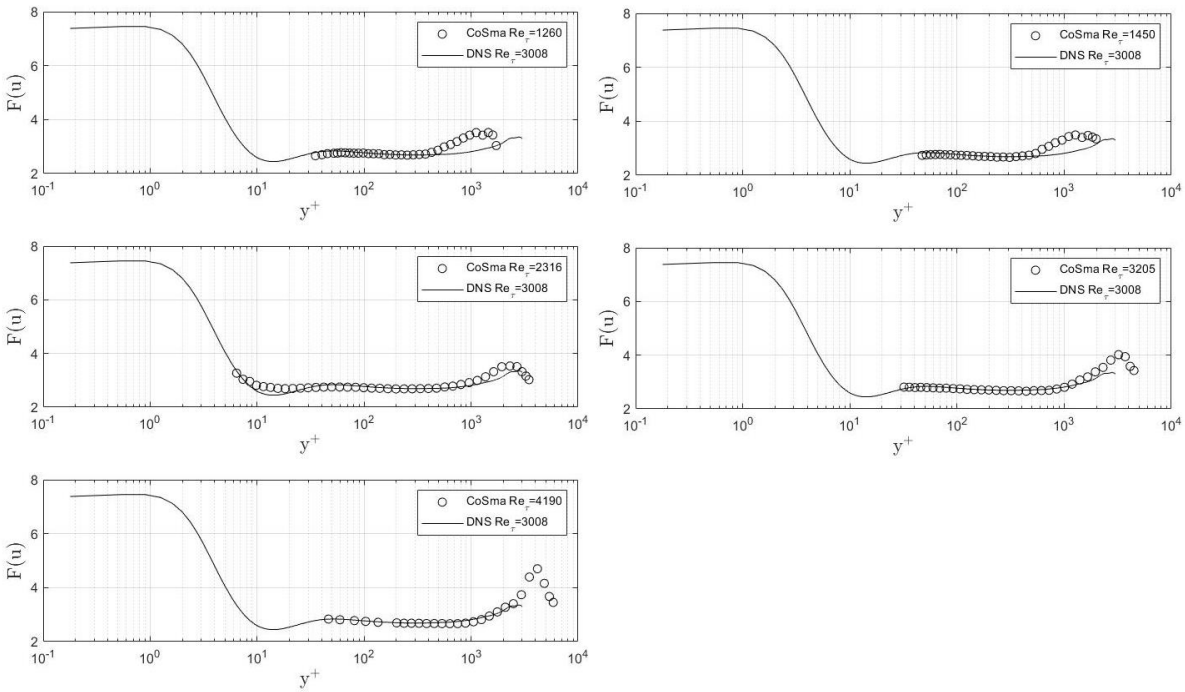

Figure 8: Kurtosis of experimental and DNS data, see Ahn et al. 2015.

Figure 8 shows better agreement between the DNS and experimental data, especially, for the higher cases which do not come by surprise due to the above mentioned proximity reason. In agreement with DNS, the experimental data remains platykurtic (negative excess kurtosis) within the log and buffer layer and gets leptokurtic (positive excess kurtosis) with increasing proximity to the centreline and within the viscous sublayer. One might observe from both Figs. 8 and 9 that both skewness and Kurtosis factors reach asymptotic values similar to value for isotropic and homogeneous turbulence, see Hinze 1975.

Conclusions and final remarks

An experimental study is progressing using the CoSma-Pipe facility at LAS, BTU C-S, to characterize pipe flow structures in fully developed turbulent flow regime over a relatively wide range of Reynolds numbers $5 \cdot 10^4 \leq Re \leq 2 \cdot 10^5$. A couple of conclusions have been drawn as follows.

The mean velocity profile indicated good agreement with the logarithmic velocity profile with constants adopted from Perry et al. 2001 as well as with recent DNS data. An inner peak for the streamwise velocity fluctuations u'^{+2} was observed in the neighborhood of y^+=15 with a maximum value between 8 and 10 depending on Reynolds number. The turbulence intensity level at the pipe centerline showed a monotonic decrease with increasing the Reynolds number. Skewness and Kurtosis factors indicated asymptotic values similar to value for isotropic and homogeneous turbulence.

Further work, no doubt, is still under progress using NSTAB, in particular, having high enough spatial resolution to remedy the unsatisfactory situation found in the literature in connection with the outer peak of the streamwise velocity fluctuations as well as the their spectral analysis.

This research work is funded within the DFG Priority Programme 1881 "Turbulent Superstructures," grant no. EG100/24-2.

References

Ahn, J., Lee, J. H., Lee, J., Kang, J.-H. and Sung, H. J., 2015: “Direct numerical simulation of a 30R long turbulent pipe flow at Re_τ = 3008,” Phys. Fluids 27.6, p. 065110. doi: 10.1063/1.4916017.

Bauer, C., Feldmann, D. and Wagner, C., 2017: "On the convergence and scaling of high-order statistical moments in turbulent pipe flow using direct numerical simulations", Physics of Fluids 29, 125105 https://doi.org/10.1063/1.4996882

Cantwell, B., Coles, D., 1983: “An experimental study of entrainment and transport in the turbulent near wake of a circular cylinder”, J. Fluid Mech. 136,321-374.

Fisher, S. N. and Hale, A. J. and Guenault, A. M. and Pickett, G. R., 2001: “Generation and Detection of Quantum Turbulence in Superfluid”, Phys. Rev. Lett. 86, pp. 244—247, doi: 10.1103/PhysRevLett.86.244

Gad-el-Hak, M., and Bandyopadhyay, P. R., 1993: “Reynolds number effect on wall-bounded flows,” Appl. Mech. Rev. 47, pp. 307–365, 1993.

Hinze, J.O., 1975: “Turbulence,” 2nd edition, McGraw-Hill, New York.

Ligrani, P. M., Bradshaw, P., 1987: “Subminiature hot-wire sensors: development and use”, J. Phys. E: Sci Instrum 20: pp. 323–332

Perry, A.E., Hafez, S., and Chong, M. S., 2001: “A possible reinterpretation of the Princeton Superpipe Data”, J. Fluid Mech. 439 395–401.

SMITS, A. J., MONTY J., HULTMARK, M., BAILEY, S. C. C., HUTCHINS N., and MARUSIC I. (2011): “Spatial resolution correction for wallbounded turbulence measurements”, Journal of Fluid Mechanics, 676, pp 4153 doi:10.1017/jfm.2011.19

Wei, T., and Willmarth, W. W. , 1989: “Reynolds number effects on the structures of a turbulent channel flow,” J. Fluid Mech. 204, pp. 57–95

Zanoun, E.-S., 2003: “Answers to some open questions in wall-bounded laminar and turbulent shear flows”, PhD thesis, Lehrstuhl für Strömungsmechanik, Universität Erlangen–Nürnberg